

Self-Similar Spatial Ordering of Clusters on Surfaces during Ostwald Ripening

G. R. Carlow and M. Zinke-Allmann

Department of Physics and Astronomy, The University of Western Ontario, London, Ontario, Canada N6A 3K7

(Received 27 January 1997)

The concept of self-similarity during late stage phase separation on surfaces will be investigated. We present the self-similar evolution of spatial ordering as a novel feature, supplementing previous discussions in the literature on scaling power laws of cluster growth and self-similar evolution of the cluster size distribution. Based on experimental data on the ripening of three-dimensional Sn clusters on Si(111) surfaces a mechanism for the observed dynamics will be discussed which is consistent with the observation of the ordering at areal cluster coverages as low as 0.1%. [S0031-9007(97)03310-3]

PACS numbers: 68.35.Fx, 68.35.Rh, 81.15.-z, 82.20.Mj

The observation of statistical self-similarity during the evolution of late stage clustering is conceptually the most intriguing feature of nonequilibrium phase separation processes. The concept is based on a comparison of distributions representing the cluster morphology at different times during the evolution process. The growth process is called self-similar if all distributions become indistinguishable upon rescaling each distribution using a single, time-dependent length scale factor. Initially a by-product of the mean-field analytical theory by Lifshitz and Slyozov (LS) for late stage Ostwald ripening [1], it has been postulated to apply to cluster *size* distributions for a wide range of dynamical processes, most clearly outlined in the seminal work by Mullins [2].

Despite (i) the increasing number of systems which seem to behave self-similarly, even including systems for which self-similar evolution is challenged, e.g., those with concurring processes such as cluster-substrate etching [3], and (ii) the improved theoretical models which take cluster-cluster interactions into account and obtain a better match with experimentally measured size distributions, we are still lacking a fundamental physical explanation of why nature chooses to proceed along self-similar paths in the evolution toward spatially separated phases. With this Letter we suggest that this is due to the fact that important features of that evolution have not been identified so far. We base this argument on a detailed study of recent data on late stage cluster ripening on surfaces where partial ordering of the nearest neighbor distance distribution has been observed [4], showing here for the first time that the evolution of these cluster *spatial* distributions is self-similar. All ripening theories in the literature, mean-field models as well as those with interactions included, assume that the relative spatial location of the clusters plays no role in the evolution of the system [5–7]. Therefore, random spatial distributions are an inherent part of these theories, and no discussion of potential spatial ordering, or the evolution of the spatial distribution, has been introduced. With the experimental finding of spatial ordering established, we will propose a model to explain this finding using the concept of local ripening as initially

introduced by Hirth [8] for the early stages of phase separation when the nucleation stage is terminated.

The experimental system for this study is Sn clustering on clean Si(111) surfaces under ultrahigh vacuum conditions since the ripening properties of this system have been characterized extensively [7,9]. Si(111) substrates were inserted into a molecular beam epitaxy facility after *ex situ* oxide growth by the Shiraki method [10]. The oxide was removed *in situ* at elevated temperature and the substrates were cooled to room temperature prior to Sn deposition from a standard effusion cell. The base pressure in the growth system was less than 5×10^{-10} Torr. All samples were *in situ* postdeposit annealed under conditions that resulted in cluster growth that is consistent with the previously observed Ostwald ripening dynamics. After cluster growth, the substrates were cooled to room temperature and removed from the growth system. The equivalent coverage of Sn on the surface in monolayers [ML, where $1 \text{ ML} = 7.8 \times 10^{14} \text{ atoms/cm}^2$ for Si(111)] was measured by *ex situ* Rutherford backscattering spectroscopy techniques. The surfaces were imaged *ex situ* with an Hitachi S-4500 field emission scanning electron microscope (SEM). The morphological parameters and growth conditions for each of the eight samples discussed in this Letter (S1–S8) are listed in Table I (equivalent Sn coverage, annealing time and temperature, and the mean cluster size, average nearest neighbor distance, and areal coverage after ripening).

A typical plane-view SEM micrograph is shown in Fig. 1(a) (sample S1). Sn clusters in the size range of about $1 \mu\text{m}$ appear as white spots on the dark Si background, with a typical 3 to $4 \mu\text{m}$ intercluster distance. The relatively narrow dispersion of cluster sizes is a characteristic of ripening-dominated growth. The spatial distribution of clusters in this micrograph is not random, but a partial ordering exists. This is seen by comparison to Fig. 1(b), which shows a random spatial configuration of clusters generated by a computer simulation using the same areal cluster density, the same average cluster size, and the same field of view as in Fig. 1(a). Note, in particular, that small nearest

TABLE I. Summary of the experimental data. All samples are Sn/Si(111). Shown for each sample, S1–S8, are the equivalent Sn coverage in monolayers, the postdeposit annealing temperature, the postdeposit annealing time, the mean cluster size (the base diameter), the average nearest neighbor spacing, the estimated areal coverage, and the scaled standard deviation of both the first and second nearest neighbor distributions.

| Sample | Equivalent coverage (ML) | Anneal temperature (°C) | Anneal time (min) | Mean cluster size (μm) | Average d_{nn} (μm) | Areal coverage (%) | $\sigma_{\text{nn}}/\langle d_{\text{nn}} \rangle \pm 0.02$ | $\sigma_{2\text{nn}}/\langle d_{2\text{nn}} \rangle \pm 0.02$ |
|--------|--------------------------|-------------------------|-------------------|-------------------------------------|---|--------------------|---|---|
| S1 | 50 | 400 | 10 | 1.0 | 3.8 | 2.4 | 0.24 | 0.18 |
| S2 | 50 | 400 | 120 | 1.7 | 7.5 | 1.8 | 0.21 | 0.17 |
| S3 | 50 | 300 | 20 | 0.7 | 4.3 | 1.2 | 0.21 | 0.19 |
| S4 | 50 | 300 | 40 | 0.9 | 6.5 | 1.1 | 0.21 | 0.17 |
| S5 | 25 | 400 | 240 | 2.1 | 20.5 | 0.41 | 0.22 | 0.18 |
| S6 | 5 | 300 | 20 | 0.8 | 12.2 | 0.17 | 0.22 | 0.19 |
| S7 | 5 | 400 | 10 | 0.7 | 15.5 | 0.16 | 0.21 | 0.18 |
| S8 | 5 | 400 | 40 | 0.9 | 18.3 | 0.12 | 0.25 | 0.17 |

neighbor distances are present in the computer simulation that do not exist in the experimental data.

To quantify this apparent spatial ordering we present the first and second nearest neighbor distance distributions. Figure 2(a) is a plot of the first nearest neighbor distribution for all samples, along with a distribution obtained for a random placement of clusters. For each distribution, the average nearest neighbor distance $\langle d_{\text{nn}} \rangle$ is rescaled to 1 and the distributions are given as probability distributions to correct for varying cluster numbers per data set. Note that the experimental data are not consistent with the random distribution nor are distances completely ordered which would lead to a delta distribution, but instead are fit well by a simple Gaussian curve. Figure 2(b) shows a plot of the second nearest neighbor distribution for all of the samples. For each distribution, the second nearest neighbor distances $d_{2\text{nn}}$ are scaled in the same way as

Fig. 2(a), i.e., using the average first nearest neighbor distances. The data for all samples overlap again on a single curve which follows again roughly a Gaussian distribution centered at a distance 28% larger than the nearest neighbor distribution. The standard deviations of the first and second nearest neighbor distributions for all samples are listed in Table I.

Note that for both distance distributions the same curve is reproduced after rescaling of all eight experimental data sets despite significant differences in growth conditions and final morphologies when the observations are recorded. As shown in Table I, this includes a variation of an order of magnitude in average cluster-cluster distances and more than one magnitude in areal coverage [11]. Variations in equivalent deposited coverage (factor of 10), annealing temperature and annealing time (varying by more than a factor of 10 at 400 °C) were required

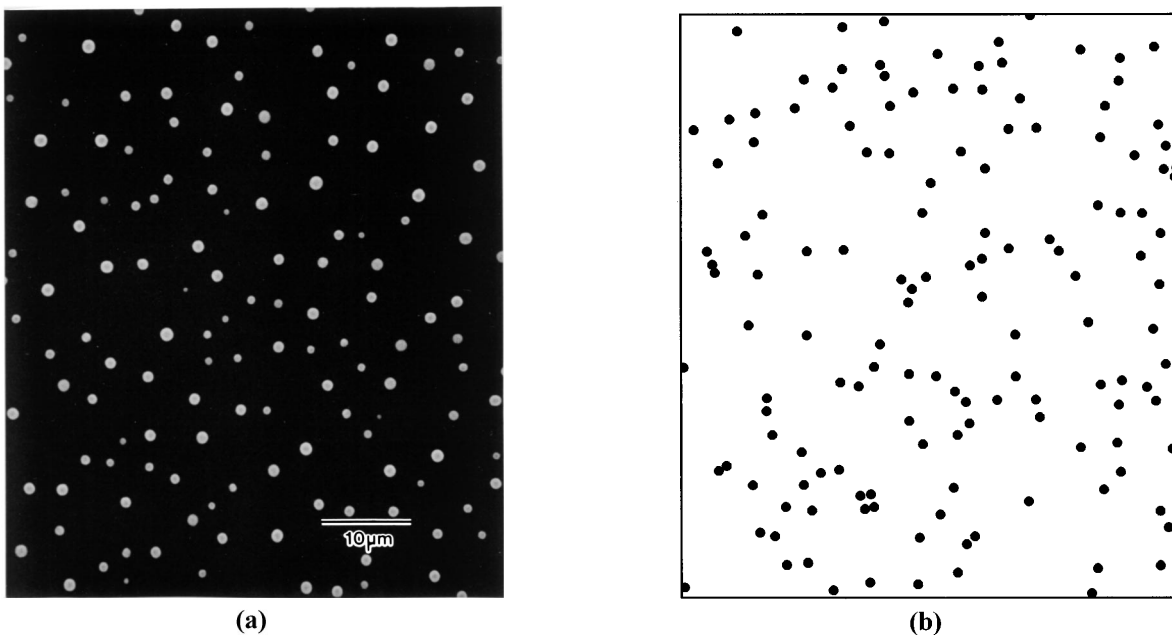


FIG. 1. (a) SEM micrograph of Sn clusters on Si(111): sample S1 (see Table I) and (b) image of a computer-generated random spatial configuration of clusters that has the same cluster density and average cluster size as the image in (a). The clusters in (a) are not randomly distributed and a partial ordering is evident.

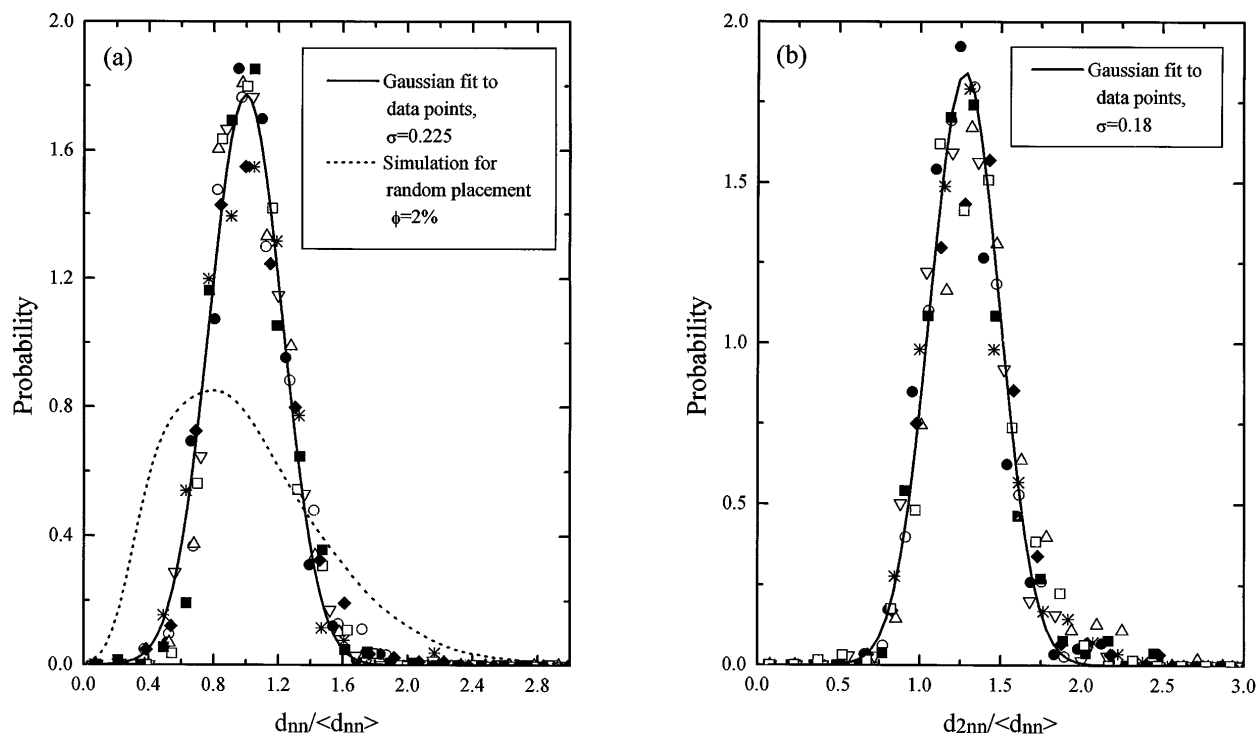


FIG. 2. Nearest neighbor distributions (a) and second nearest neighbor distributions (b) for samples S1–S8 [S1 (◆), S2 (■), S3 (▽), S4 (●), S5 (○), S6 (△), S7 (□), S8 (*)]. All distances for each sample are measured relative to their average nearest neighbor distances. In this representation, all of the data coincide on the same curves (solid lines). A nearest neighbor distribution for a random spatial arrangement of clusters is shown as the dotted line in (a).

to achieve these variations. We use Mullin's definition of self-similarity, $f(r, t) = f\{[r^*(\lambda t)/r^*(t)]r, \lambda t\}$ [2], where $f(r, t)$ is the distribution function depending on a length scale parameter r and the time t , and where r^* is an average value of this parameter at times t and λt . From this we conclude that the entire evolution of clusters in the late stage develops with a self-similar spatial distribution of clusters and that one distribution differs from another by a simple scaling factor—the average nearest neighbor distance.

Note further that the mechanism of partial spatial ordering cannot be confined to the very early stages of growth, but must instead persist throughout the late stages. This is illustrated for samples S1 and S2 whose scaled nearest neighbor distributions are shown again in Fig. 3. Note from Table I that these samples only differ with respect to annealing time, thus statistically representing two subsequent snapshots (S1 at 10 min and S2 at 120 min) in the evolution of a ripening system. If the ordering mechanism would be a memory effect from the early stages of clustering (as, e.g., discussed and defined in Ref. [7]), then the evolution between snapshots S1 and S2 would have to develop in a way that randomly selects clusters that survive the ripening process. We have taken the spatial distribution from S1 and randomly eliminated the proper number of clusters to obtain the areal cluster number distribution of sample S2. This process was repeated until a consistent prediction of the next nearest cluster size distribution was obtained, shown

as the solid line in Fig. 3. Note that this distribution is not consistent with the experimental distribution of S2, also shown in that figure. Therefore, the dissolution of clusters between S1 and S2 is not random and instead selective dissolution of smaller clusters occurs such that the spatial distribution evolves in a self-similar fashion.

As self-similarity for both the cluster size distribution [9] and cluster spatial distribution occurs at the same time, we need just one mechanism responsible for both the global ripening and the ordering processes. Since it has been well established that diffusion driven ripening describes the ripening of the Sn/Si(111) system under the conditions presented in this study (Table I), a diffusion limited mechanism should also hold for the spatial ordering. Further, the mechanism has to be consistent with the observation that the n th nearest neighbor distribution can be expressed as $g_n(d, t) = g_n\{[d_1^*(\lambda t)/d_1^*(t)]d, \lambda t\}$, where $d_1^*(t)$ is the average first nearest neighbor spacing at time t , and $d_n^*(t) \propto t^{3/8}$, for all n based on ripening dynamics for the mixed geometry [12]. Specifically, for our experiments, the function g_1 must be consistent with a simple Gaussian distribution centered at 1 with a standard deviation of $\sigma_{nn} = 0.23$.

A mechanism which may be compatible with all these requirements is local ripening. This effect is very similar to the Ostwald ripening mechanism, as it also is based on three effects, the mass conservation condition, surface diffusion as the mass transport mechanism, and the Gibbs-Thomson effect [13] favoring larger clusters over smaller

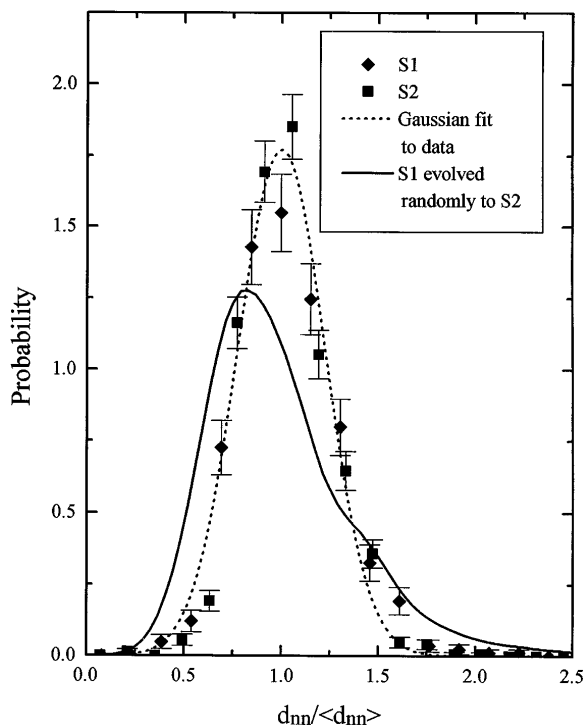


FIG. 3. The nearest neighbor distributions for $S1$ (\blacklozenge), $S2$ (\blacksquare), and $(-)$ for the computer simulation where $S1$ evolves to $S2$ by a random dissolution of clusters. The disagreement indicates that, during the evolution of $S1$ towards $S2$, selective dissolution of clusters occurs.

ones. The only difference is that in Ostwald ripening the diffusion equation is not spatially directed in a mean-field approach, while in local ripening the diffusion gradient is developed between two neighboring clusters. The similarity of the two effects allows us to assume that including local ripening in the description of the system does not alter the fact that only one length scale dominates the process, while it explains at the same time the preferential elimination of near cluster pairs as observed in the experiments. Also favoring local ripening as the explanation of the above observations are indications that the morphology of the system alters toward a more random cluster spatial distribution (associated with narrower, more LS-like cluster size distributions) when fluctuations in the adatom concentration are introduced which effectively eliminate the development of long-ranging diffusion gradients across the surface. This has been demonstrated recently [4] for cluster growth occurring under low deposition rates, i.e., deposition rates small enough that the system does not become coalescence dominated.

In summary, we have observed that during ripening dominated cluster growth on surfaces the spatial arrangement of clusters exhibits partial ordering and that the cluster spatial distribution evolves in a self-similar fashion over a wide range of areal coverages and average cluster-cluster distances. The ordering is observed at areal coverages as low as 0.1%. We suggested local ripening as the mechanism responsible for the spatial ordering which therefore becomes a process which has to be included more consistently also in late stage cluster growth simulations and modeling.

This work was carried out with funding from Natural Sciences and Engineering Research Council of Canada.

-
- [1] I. M. Lifshitz and V. V. Slyozov, *Sov. Phys. JETP* **35**, 331 (1959).
 - [2] W. W. Mullins, *J. Appl. Phys.* **59**, 1341 (1986).
 - [3] T. D. Lowes and M. Zinke-Allmang, *J. Appl. Phys.* **73**, 4937 (1993); *Phys. Rev. B* **49**, 16 678 (1994).
 - [4] G. R. Carlow, R. Barel, and M. Zinke-Allmang (to be published).
 - [5] J. A. Marqusee and J. Ross, *J. Chem. Phys.* **80**, 536 (1984); B. K. Chakraverty, *J. Chem. Phys. Solids* **28**, 2401 (1967).
 - [6] Note that the ripening concept has recently been connected with a kinetic rate equation model for three-dimensional systems; see J. B. Adams and W. G. Wolfer, *Acta Metall. Mater.* **41**, 2625 (1993).
 - [7] M. Zinke-Allmang, L. C. Feldman, and M. H. Grabow, *Surf. Sci. Rep.* **16**, 377 (1992).
 - [8] J. P. Hirth, *J. Cryst. Growth* **17**, 63 (1972).
 - [9] G. R. Carlow and M. Zinke-Allmang, *Surf. Sci.* **328**, 311 (1995); R. Barel, Y. Mai, G. R. Carlow, and M. Zinke-Allmang, *Appl. Surf. Sci.* **104/105**, 669 (1996).
 - [10] A. Ishizaka and Y. Shiraki, *J. Electrochem. Soc.* **133**, 666 (1986).
 - [11] The areal coverage cannot be too large since this results in concurrent ripening and coalescence, and this alters both the spatial and cluster size distributions (see Ref. [4]).
 - [12] The predicted exponent of $\frac{3}{8}$ for the time evolution of the nearest neighbor distance follows directly from the cluster growth law $r^4 \propto t$ (see Ref. [7]), and the mass conservation condition $nr^3 = \text{const}$, where n is the number of clusters per unit area. Taking $n \approx 1/d^2$, where d is a typical distance between clusters, then $d \propto t^{3/8}$.
 - [13] J. W. Gibbs, *Trans. Connect. Acad.* **3**, 108 (1876); W. Thomson, *Philos. Mag.* **43**, 448 (1871).